10-1-2001

Observations of Persistent Leonid Meteor Trails. 1. Advection of the "Diamond Ring"

Jack D. Drummond

Brent W. Grime

Chester S. Gardner

Alan Z. Liu
Embry Riddle Aeronautical University - Daytona Beach, liuz2@erau.edu

Xinzhao Chu

See next page for additional authors

JOURNAL OF GEOPHYSICAL RESEARCH, VOL. 106, NO. A10, PAGES 21,517-21,524, OCTOBER 1, 2001

Observations of persistent Leonid meteor trails 1. Advection of the "Diamond Ring"

Jack D. Drummond and Brent W. Grime
Starfire Optical Range, Directed Energy Directorate, Air Force Research Laboratory, Kirtland Air Force Base, New Mexico

Chester S. Gardner, Alan Z. Liu, and Xinzhao Chu
Department of Electrical and Computer Engineering, University of Illinois at Urbana-Champaign, Urbana, Illinois

Timothy J. Kane
Department of Electrical Engineering, The Pennsylvania State University, University Park, Pennsylvania

Abstract. From a single image of a persistent trail left by a -1.5 magnitude Leonid meteor on November 17, 1998, the relative winds between 92.5 and 98 km altitude are derived, where the altitudes are determined by a sodium lidar. These are converted to true winds 82 sec after the appearance of the meteor by fixing the winds at 98 km to match the results of following the trail with the lidar for twelve minutes. The image and winds reveal a fine example of the effects of a gravity wave having a vertical wavelenth of 5.50 ± 0.02 km, a horizontal wavelength of 2650 ± 60 km, an intrinsic period of 19.5 ± 0.4 hours, and an observed period of 8.6 ± 0.1 hours. Effects of the gravity wave are still present in the wind field 70 min later.

1. Introduction

The 1998 Leonid meteor shower provided an opportunity to study the lingering trails left by some of the brighter meteors, trails that were visible for more than 20 min and could be tracked by lidar for even longer [*Chu et al.*, 2000]. Lingering or persistent meteor trails can last up to an hour and have been recorded throughout history. They were first reported in the scientific literature following the Leonid meteor showers of November 1866-1868. See, for example, the very first volume of *Nature* [*Lockyer*, 1869]. Persistent trails are still a mystery more than a century later. We begin a series of papers analyzing the trails produced by the Leonids in 1998 and 1999 with a study of the wind field at their altitude by a new method, new because it uses the known atmospheric trajectory of the meteor. Observations of persistent trails can only be planned to the extent that they can be predicted (to some degree) to occur for a few years around the time of the Leonid meteor storms every 33 years. In 1998 a strong fireball peak occured on November 17, some 12 hours before the main peak of fainter meteors. Altogether, we obtained videos [*Drummond et al.*, 1999] and recorded observations of seven lingering trails on this night and two more the following year, on November 19, 1999. Two lasers were used in 1998 at the Starfire Optical Range (SOR), a facility owned by the Directed Energy Directorate of the Air Force Research Laboratory. One, a copper vapor laser, attempted to produce backscatter from a trail. A CCD camera attached to a 400 mm lens was used to look for this backscatter, and although none was recorded, a spectacular image (Plate 1) was obtained of the first lingering trail. Dubbed the Diamond Ring for its appearance, the trail was visible to the naked eye for 5 min. Taken 82 s after the meteor was seen, the one (and unfortunately only) image of the trail shows a loop caused by the effects of a gravity wave on the wind field.

The other laser, part of a sodium resonance lidar system, was highly productive, and the results of that experiment for the seven trails are reported elsewhere [*Chu et al.*, 2000; *Kelley et al.*, 2000; *Grime et al.*, 2000]. *Drummond et al.* [2000] and Kelley et al. describe the visual observing procedures, Chu et al. describe the sodium lidar experiment, and Grime et al. derive winds by tracking the trails. The current paper is the first in a series detailing the results of studying the Leonid lingering trails of 1998 and 1999. The second paper in our series [*Kruschwitz et al.*, this issue] reports on the photometry derived from the CCD image (Plate 1) of the Diamond Ring. Other papers in the series will cover the results for another trail observed in 1998, the Glowworm, and two trails in observed in 1999, the Puff Daddy and the French Curve.

Paper number 2000JA000173.
0148-0227/01/2000JA000173$09.00

The lidar, in its normal stare mode, provides information along its line of sight on the number density, temperature, and velocity of neutral sodium atoms, from which winds can also be derived at the altitude of the naturally occuring layer between 80 and 100 km. For this experiment, when a meteor left a lingering trail, a visual observer called out its elevation and azimuth, directing the 3.5 m telescope to the trail's position. The telescope's 3.5 m mirror was used both as the lidar's transmitter and receiver. A video camera, mounted on the telescope's superstructure, recorded a 5° field centered on the telescope/lidar pointing. The CCD was located on a separate mount some 50 m from the 3.5 m telescope but could follow the pointing of the telescope. All recordings would begin within about a minute of the meteor's appearance, at which time the lidar would measure a great enhancement of sodium in a portion of the trail at a specific altitude. Between the lidar display and video monitor, scientists in the telescope control room could track the trail, redirecting the telescope long after the trail faded from the view of the visual observers. Unfortunately, computer problems with the CCD limited the number of images obtained during 1998. Visual magnitudes of the meteors were independently estimated by two observers, who never disagreed by more than half a magnitude. Since both Jupiter and Saturn were available, in addition to the bright stars in the winter constellations, meteor magnitudes could be estimated by interpolating between stars or planets to as bright as magnitude -2.5.

2. Trajectory and Trail

The loop in the Diamond Ring makes a clean ellipse (Figure 1), with the small axis directed at the zenith. The lidar registered returns from two altitudes in its line of sight, the centers of Plate 1 and Figure 1. In this direction, marked by the intersection of the ellipse and the extension of the lidar beam in Figure 1, portions of the trail at 98 and 92.5 km appear to overlap or

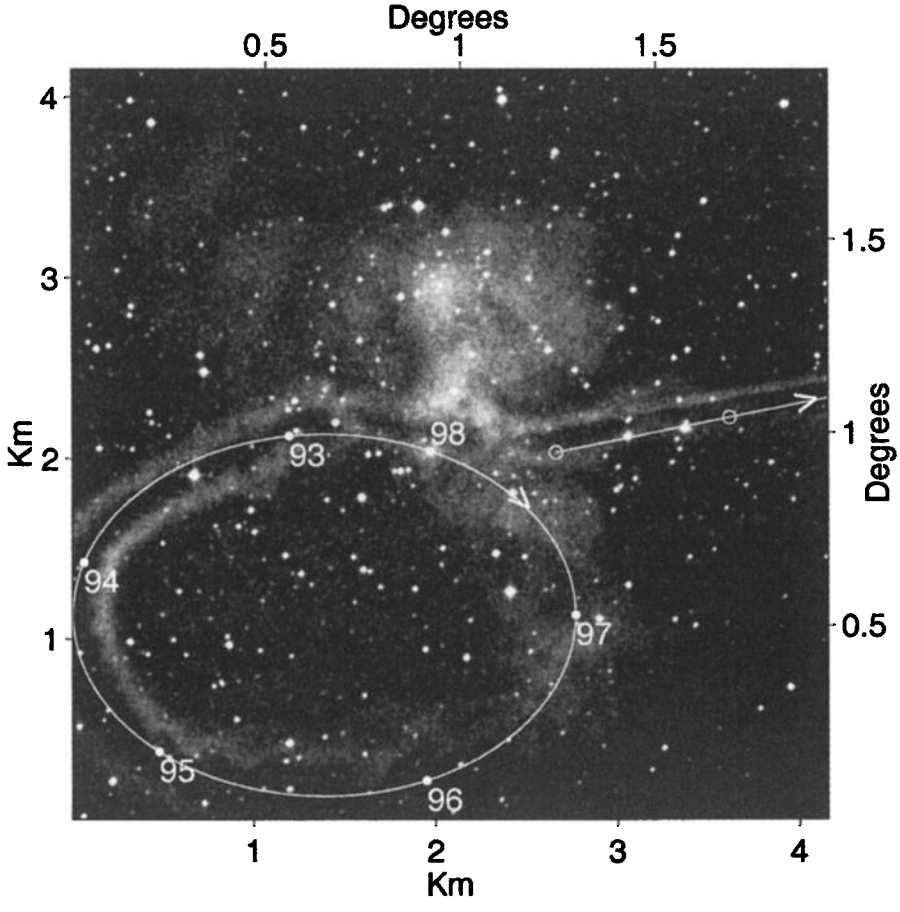

Figure 1. The arrowed straight line theoretical trajectory of a Leonid and the loopy part of its trail 82 s later. The highest part of the meteor trail is at the upper left. It makes a loop as it descends, and the lowest portion of the trail is at the right, nearly along the original trajectory, which by coincidence, lies just below and parallel to the lidar beam, which is emerging from the right side of the camera field and disappears at the center. The direction to the zenith is at the top, and increasing azimuth is to the right. Altitudes are shown at various points along the trail. After adjusting the theoretical trajectory of a Leonid for the winds, the two circles, from left to right on the arrow trajectory, mark the starting points corresponding to the end points on the trail at 98 and 97 km altitude.

Plate 1. The Diamond Ring. Eighty two seconds after a -1.5 magnitude Leonid meteor appeared over Albuquerque at 0228 LT on November 17, 1998, its trail has been contorted into the appearance of a Diamond Ring. The 1 W sodium laser is the straight streak coming in from the right. The 502 pixel field of view is 1.94° in this image, taken at an azimuth of 128° and an elevation angle of 51°. The scale of the image is obtained from the field of view and the known (from the lidar) mean slant range of 122.6 km.

cross each other. Because the two altitudes at the overlap point on the ellipse are known, the true path of the loop between 98 and 92.5 km in the sky is fixed, having a vertical wavelength of 5.5 km. Assuming further that the vertical wind is small and does not vary between these altitudes allows the ellipse to be fit by a parametric curve where the image coordinates X' and Y' are expressed as functions of altitude Z, all in kilometers:

$$X' = 1.39 + 1.38 \sin[(98.38 - Z)2\pi/5.5]$$
$$Y' = 1.13 + 1.00 \cos[(98.38 - Z)2\pi/5.5] . \quad (1)$$

The theoretical trajectory of a Leonid is also known for a given time and is translated to the field of Figure 1 (which shows the trajectory after adjusting for the winds, as determined below). Rotating the image coordinates to true, results in Figure 2, an illustration of the trajectory and the trail in true coordinates.

3. Relative and True Winds

Subtracting the XYZ components of the looping path from the components of the theoretical trajectory and dividing by the 82 s between the appearance of the meteor and the time of the image gives the three components of the relative wind as a function of altitude. By following the changing elevation and azimuth of the lidar return from the 98 km altitude section of the Diamond Ring for 12 min, beginning 9 min after the image (Plate 1) was obtained, *Grime et al.* [2000] were able to determine the true wind components UVW at 98 km altitude. Fixing our relative winds to their values at this height then yields the true wind components at all altitudes from the single image of the distorted trail, assuming that the winds at 98 km have not changed during the 22 min between the time of the appearance of the meteor and the conclusion of tracking the trail.

Figure 3 shows the winds as a function of altitude as determined by this method and from routine lidar measurements made 1 hour and 10 min after the image. This latter wind field is derived from converting sodium lidar measurements of the radial wind component in the four cardinal directions 15° from the zenith to UVW components [*Bills et al.*, 1991; *Grime et al.*, 2000; *Chu et al.*, 2000].

With the true wind at the time of the Diamond Ring now known, the U and V components can be expressed

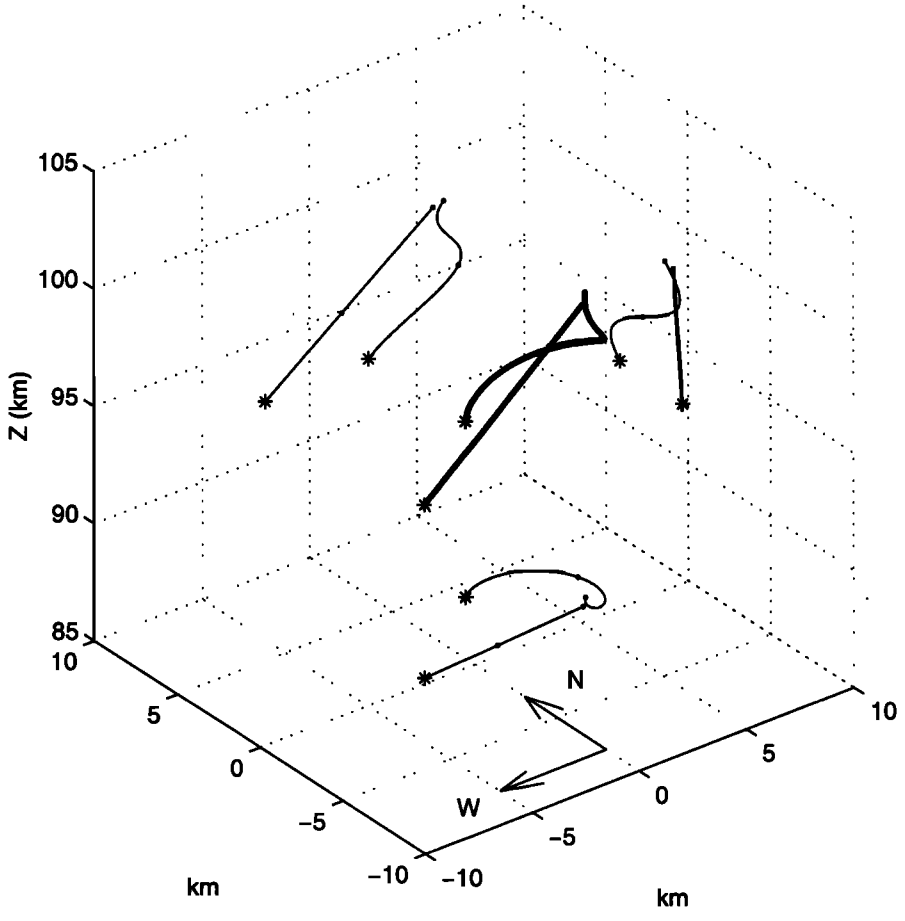

Figure 2. Three-dimensional representation of the trajectory and trail. The thick straight line shows the initial trajectory, and the loopy thick line shows the trail 82 s later. The thin lines are the projection of these two onto the ground, the vertical and N-S plane, and the vertical and E-W plane. Asterisks mark the bottom of the trajectory and trail.

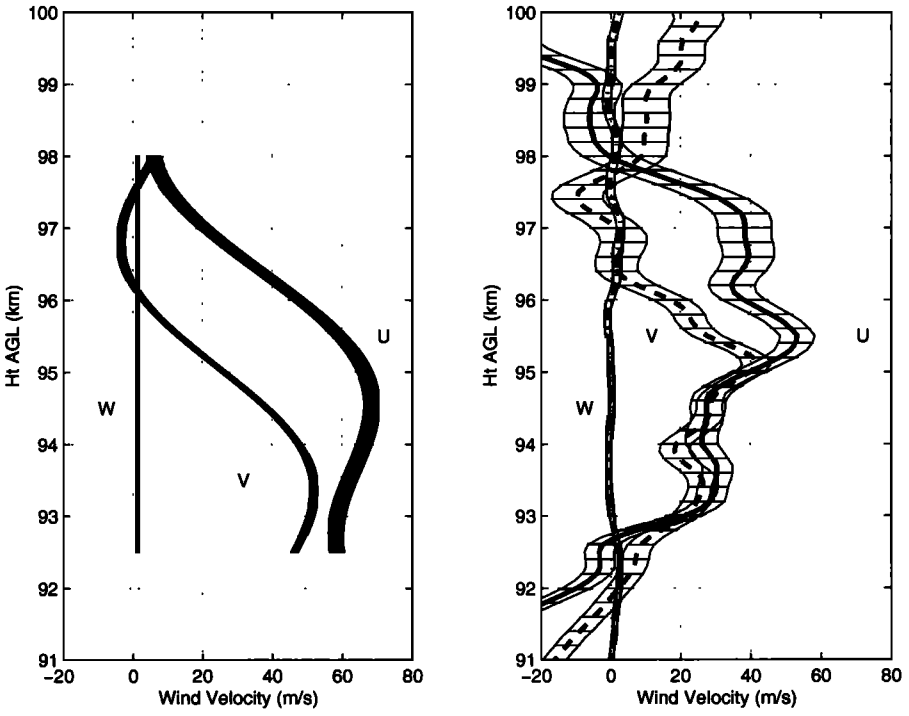

Figure 3. The wind field as a function of altitude. Positive U corresponds to the eastward (zonal) component, positive V corresponds to the northward (meridional) component, and positive W corresponds to the vertically upward component. (left) Wind components as determined from the difference between the theoretical trajectory and the trail, where the thickness of the lines corresponds to the uncertainty determined at 98 km by *Grime et al.*, [2000]. (right) Wind components as determined from lidar 70 min later, shown with horizontal error bars.

as a function of true altitude Z. Simultaneously fitting U and V (m s^{-1}) as a function of Z (km) yields

$$U = 961 - 9.59Z + 16.13\cos[(Z - 95.02)2\pi/5.5]$$

$$V = 721 - 7.33Z - 16.41\sin[(Z - 95.08)2\pi/5.5]\,. \quad (2)$$

Both (1) and (2) are parametric forms of the equation of an ellipse in the horizontal plane, and since the loop in the trail is fit so well with an ellipse, no higher terms are required. However, note the strong periodic component in the last terms of U and V. Figure 4 shows U and V and the extracted periodic and nonperiodic components of the wind. Over a height range of 5.5 km the periodic component vector traces out an ellipse with semiaxes 16.8 x 15.7 m s^{-1}, with the major axis aligned 38° east of north. The nonperiodic component vector traces out a straight line that makes an angle of 37° with north and increases in velocity with depth.

Fitting the wind field derived 70 min later from the lidar data with (2), where the 5.5 km vertical wavelength is maintained, results in Figure 5 which presents the same information as Figure 4 for the Diamond Ring. The equations expressing the horizontal wind field from the lidar data are

$$U = 2 + 0.29Z + 15.63\cos[(Z - 95.57)2\pi/5.5]$$

$$V = 213 - 2.07Z - 14.89\sin[(Z - 96.14)2\pi/5.5]\,. \quad (3)$$

It appears that a vertical wavelength of 5.5 km is still present in the wind field but is accompanied by additional components with smaller vertical wavelengths. The other main difference between Figures 4 and 5 is the decrease in the linear component velocity at the lowest altitudes at the later time.

In summary, to illustrate the effects of the wind, Figure 6 shows the sequence of the development of the Diamond Ring from start to finish, from the trajectory to the image.

4. Gravity Wave

Assuming that the elliptical loop in the Diamond Ring trail and the periodic component of the wind are manifestations of a quasi-monochromatic gravity wave [*Hines*, 1960], we begin the examination of the nature of the gravity wave by noting that the inertial, or Coriolis, frequency for the SOR at latitude $\phi = +35°$ is $\omega_{\text{inertial}} = 2\ \Omega\ \sin\phi = 8.358 \times 10^{-5}$ s^{-1}, where Ω is the sidereal frequency of the Earth's rotation, 7.292×10^{-5} s^{-1}. The buoyancy frequency squared is given by $N^2 = g/T\ (dT/dZ + g/C_p)$, where $g = 9.52$ m s^{-2} is the gravitational acceleration at $Z = 95$ km altitude, $T = 183.5°$ K is the mean temperature as mea-

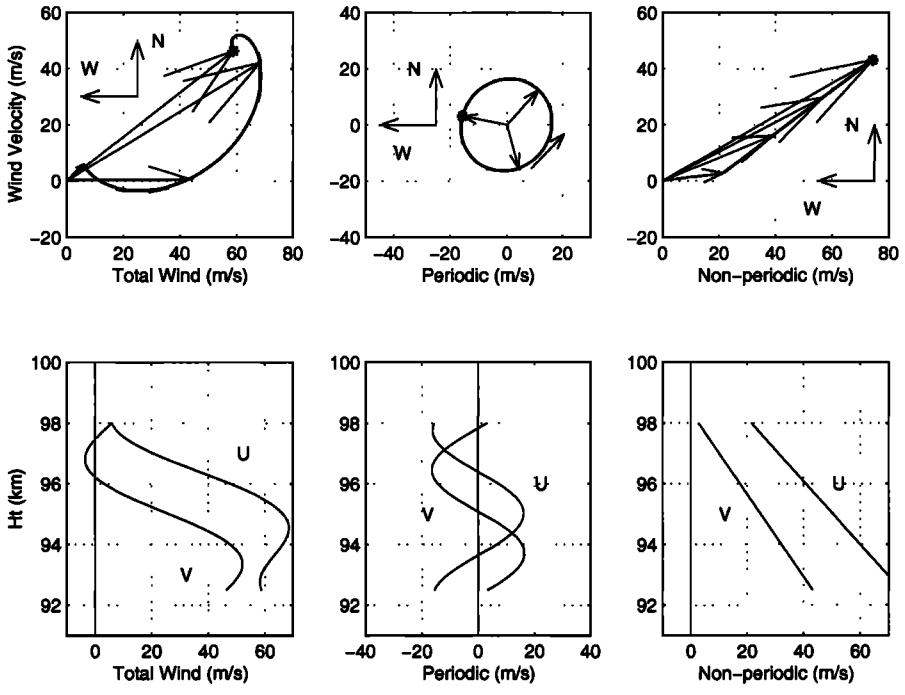

Figure 4. The U and V components of the wind and their periodic and nonperiodic components. (top) U and V, and their components, are projected onto the ground. The asterisks indicate the lowest altitude. The periodic component causes the wind to rotate in a counterclockwise (NWSE) direction with decreasing altitude, while the nonperiodic wave component is an overall northeastwardly wind that also turns counterclockwise (from 83° to 60°) while increasing greatly in strength with depth into the atmosphere. (bottom) U and V, and their components, are plotted as function of altitude.

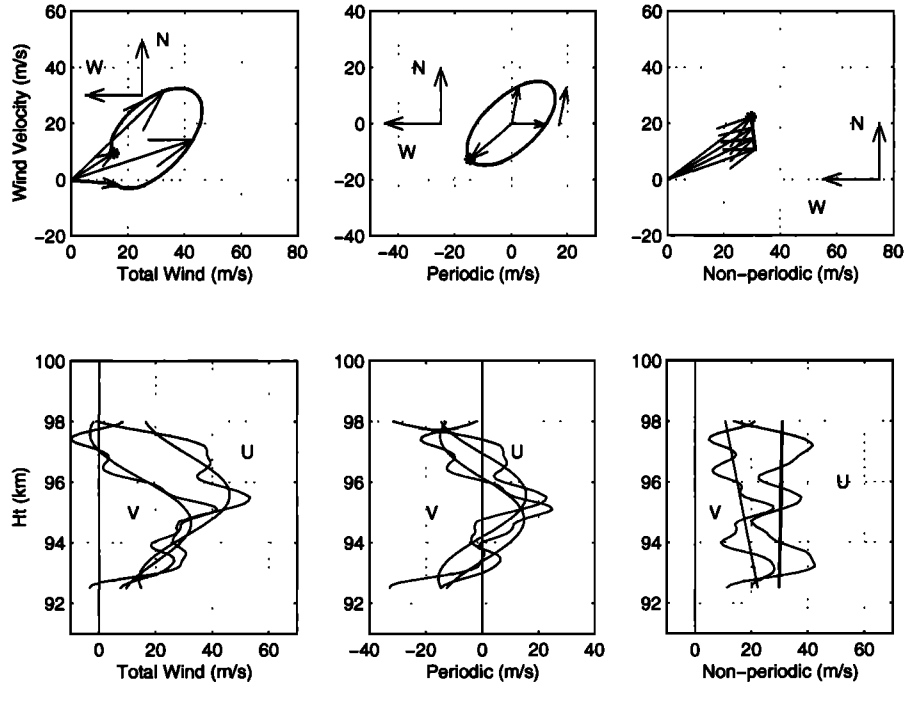

Figure 5. The same as Figure 4, but the wind field is found near the zenith from lidar 70 min after the Diamond Ring: (top) Only the fit of the lidar data with (2) is shown; (bottom) both the fitted and measured wind components are shown. The fits are made with the 5.5 km vertical wavelength found for the Diamond Ring. Note how the linear component wind velocity has decreased at lower altitudes since the Diamond Ring.

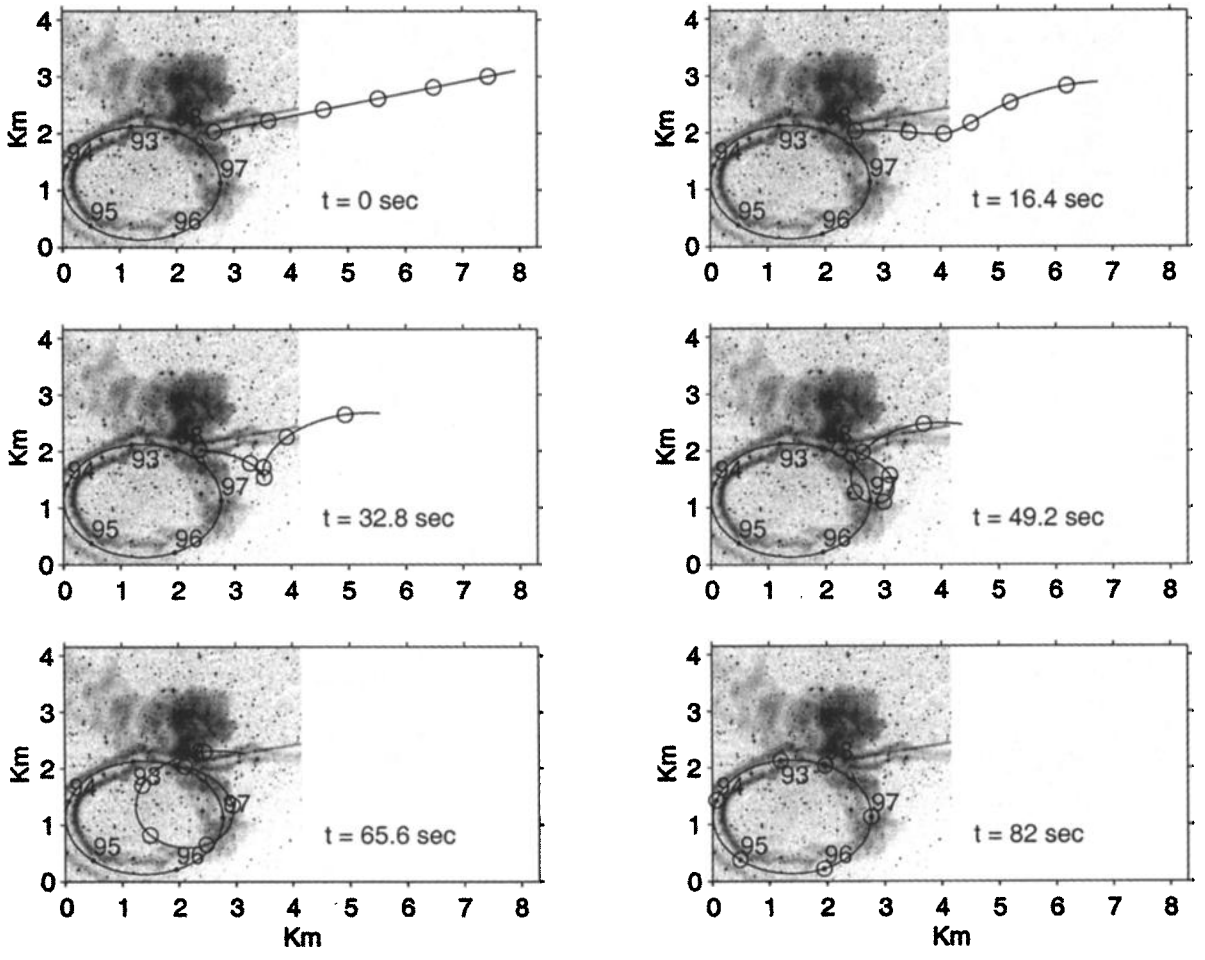

Figure 6. Production of the Diamond Ring. Starting from the original trajectory, the development of the Diamond Ring is traced to its appearance in Plate 1. See text.

sured by the lidar, and $C_p = 1004$ J (° kg)$^{-1}$ is the specific heat under constant pressure. Using the measured lapse rate of $-dT/dZ = 4.9°$ km^{-1}, $N^2 = 2.37 \times 10^{-4}$ s^{-2}.

The intrinsic frequency for the loop is $\omega_{\text{int}} = \omega_{\text{inertial}} \times a/b = 8.943 \times 10^{-5}\text{s}^{-1}$, where a/b is the ratio of major to minor axes of the periodic component of the gravity wave, 16.8/15.7. The horizontal wave number k can be

Table 1. Gravity Wave Wind Parameters

Parameter	Value
Observed or measured	
Temperature	183.5±0.7°K
Vertical wavelength	5.50±0.02 km
Vertical wave number	11.42±0.05 × 10^{-4} m^{-1}
Mean wind speed at Z=95.25 km along 38°	47.6±0.25 m s^{-1}
ω_{inertial}	0.8358×10^{-4}s^{-1} (τ = 20.88 hours)
Calculated	
Buoyancy frequency N	154.0±3.0 × 10^{-4}s^{-1} ($\tau = 6.80 \pm 0.13$ min)
ω_{observed}	2.022±0.030 × 10^{-4}s^{-1} ($\tau = 8.63 \pm 0.13$ hours)
$\omega_{\text{intrinsic}}$	0.8943±0.0175 × 10^{-4}s^{-1} ($\tau = 19.52 \pm 0.38$ hours)
Scale height	5.530±0.021 km
Horizontal wave number	0.0237 ± 0.0005 × 10^{-4} m^{-1}
Horizontal wavelength	2652 ± 56 km

found from inverting the dispersion relation of acoustic gravity waves [*Hines*, 1960],

$$k^2 = (m^2 - \omega_{\rm int}^2/C_s^2 + 0.25/H^2)(\omega_{\rm int}^2 - \omega_{\rm inertial}^2) \Big/ (N^2 - \omega_{\rm int}^2) = 5.612 \times 10^{-12}{\rm m}^{-2} , \quad (4)$$

where $m = 1.142 \times 10^{-3}$ m^{-1} is the vertical wave number for the observed vertical wavelength of 5.5 km, $H = 5.530 \times 10^3$ m is the calculated scale height, and $C_s = \sqrt{\gamma g H} = 271.5$ m s^{-1} is the calculated speed of sound at 95 km altitude for $\gamma = 1.4$ (the ratio of specific heat at constant pressure to specfic heat at constant volume).

The observed frequency for the loop is

$$\omega_{\rm obs} = \omega_{\rm int} + k\ U_r = 2.022 \times 10^{-4}{\rm s}^{-1} , \quad (5)$$

where $U_r = 47.6$ m s^{-1} is the nonperiodic wind velocity at the mean altitude of 95.25 km in the direction of propagation of the wave 38° east of north, along the major axis of the periodic component of the gravity wave. Since the periodic component of the wave is very nearly circular, the loop in the Diamond Ring is caused primarily by a low-frequency wave with a very shallow propagating angle, traveling over the SOR in a northeastwardly direction and originating from a distant location. The various parameters are summarized in Table 1, including the periods τ derived from the frequencies.

5. Summary

We report a unique method of obtaining the wind field at lower thermospheric altitudes from a meteor trail. The wind field between 92.5 and 98 km altitude is found in five steps: (1) The intitial atmospheric trajectory of the parent meteor is known, in this case a Leonid. (2) A single image of the trail (the Diamond Ring) is obtained 82 seconds later. (3) A sodium lidar provides altitude information for portions of the trail. (4) The trail is fit with an analytical expression. (5) Finally the wind field is adjusted to match that at a single altitude found from tracking the trail.

The relative wind field is found by comparing the meteor trajectory and the analytic expression for the trail obtained from the single image, using the altitude information from the lidar. Tracking the trail leads to the wind field at a single altitude, 98 km, and in turn provides a zero point to convert the relative to true winds over a range of altitudes. The wind field found here, especially the periodic component, is for the most part still present 70 min later.

The analytic expression for a portion of the trail is possible because it forms a virtually perfect apparent ellipse between 92.5 and 98 km, indicating the presence of but a single perturbing influence. This ellipse is a manifestation of a low intrinsic frequency (19.52 hour period) gravity wave having a vertical wavelength of 5.5 km and a horizontal wavelength of 2652 km. Thus the Diamond Ring has provided gravity wave wind parameters normally obtained only from rocket launches, [e.g., *Larson*, 2000].

Acknowledgments.
Janet G. Luhmann thanks both of the referees for their assistance in evaluating this paper.

References

Bills, R. E., C. S. Gardner, and C. Y. She, Narrowband lidar techniques for sodium temperaure and Doppler wind observations of the upper atmosphere, *Opt. Eng.*, *30*, 13-21, 1991.

Chu, X., A. Z. Liu, G. Papen, C. S. Gardner, M. C. Kelley, J. Drummond, and R. Fugate, Lidar observations of elevated temperatures in bright chemiluminscent meteor trails during the 1998 Leonid shower, *Geophys. Res. Lett.*, *27*, 1815-1818, 2000.

Drummond, J., M. C. Kelley, and C. S. Gardner, Leonid trails and lasers, video presented at Asteroids, Comets, Meteors III, Cornell Univ, Itahaca, N.Y., July 26-30, 1999.

Drummond, J., C. S. Gardner, and M. C. Kelley, Catching a falling star, *Sky Tel.*, *99*, 46-49, 2000.

Grime, B. W., T. J. Kane, A. Liu, G. Papen, C. S. Gardner, M. C. Kelley, C. Kruschwitz, and J. D. Drummond, Meteor trail advection observed during the 1998 Leonid shower, *Geophys. Res. Lett.*, *27*, 1819-1822, 2000.

Hines, C. O., Internal atmospheric gravity waves at ionospheric heights, *Can. J. Phys.*, *38*, 1441-1481, 1960.

Kelley, M.C., et al., First observations of long-lived meteor trains with resonance lidar and other optical instruments, *Geophys. Res. Lett.*, *27*, 1811-1814, 2000.

Kruschwitz, C. A., et al., Observations of persistent meteor trails, 2. Photometry and numerical modeling, *J. Geophys. Res.*

Larsen, M., Coqui II: Mesospheric and lower thermospheric wind observations over Puerto Rico, *Geophys. Res. Lett.*, *27*, 455-448, 2000.

Lockyer, N., Editorial note, *Nature*, *1*, 58, 1869.

X. Chu, C. S. Gardner, and A. Liu, Department of Electrical Engineering, University of Illinois at Urbana-Champaign, Urbana, Ill 61801.

J. D. Drummond and B. W. Grime, Starfire Optical Range, Directed Energy Directorate, Air Force Research Laboratory, 3550 Aberdeen Av SE, Kirtland AFB, NM 87117. (jack.Drummond@kirtland.afmil)

T. J. Kane, Department of Electrical Engineering, Pennsylvania State University, University Park, PA 16802.

(Received May 16, 2000; revised February 13, 2001; accepted February 13, 2001.)